

# Gas foaming of polyphenyl sulfone: Effect of the blowing agents and operating parameters

Paolo Trucillo<sup>1,2</sup>  | Fabrizio Errichiello<sup>1,3</sup>  | Ernesto Di Maio<sup>1,2</sup> 

<sup>1</sup>Foamlab, University of Naples Federico II, Naples, Italy

<sup>2</sup>Dipartimento di Ingegneria Chimica, dei Materiali e della Produzione Industriale, University of Naples Federico II, Naples, Italy

<sup>3</sup>Materias S.R.L., Naples, Italy

## Correspondence

Paolo Trucillo, Dipartimento di Ingegneria Chimica, dei Materiali e della Produzione Industriale, University of Naples Federico II, P. le Tecchio 80, I-80125, Napoli, Italy.

Email: [paolo.trucillo@unina.it](mailto:paolo.trucillo@unina.it)

## Abstract

Polyphenyl sulfone (PPSU) is a highly stable and rigid polymer with good chemical and mechanical resistance used in automotive and aerospace industries in high-temperature applications during long-operating cycles. PPSU foams are applied as core materials in lightweight composites ensuring high strength, fire resistance, thermal and acoustic insulation. In this paper, PPSU slabs are foamed using CO<sub>2</sub>, N<sub>2</sub>, and He as blowing agents (BAs). An experimental campaign is carried out to estimate the BAs' diffusivity in the polymer. In details, CO<sub>2</sub> diffusivity ranges from 8E-11 to 1E-09 m<sup>2</sup>/s at temperatures from 220 to 260°C; diffusivity of N<sub>2</sub> ranges from 2E-10 to 5E-09 m<sup>2</sup>/s (220–260°C) and it is 4E-09 m<sup>2</sup>/s for He at 220°C. Foaming tests reveal an expansion ratio as high as 400% for CO<sub>2</sub>, 130% for He, and 150% for N<sub>2</sub>. Scanning electron microscopy analysis is also performed on produced samples, obtaining a cell number density of 1.3E07, 2.6E05, and 1.8E06 cells/cm<sup>3</sup> when saturating, respectively, with CO<sub>2</sub> at 220°C and 100 bar, N<sub>2</sub> at 220°C and 100 bar, and He at 230°C and 100 bar.

## KEYWORDS

blowing agents, foams, gas-foaming, polysulfones

## 1 | INTRODUCTION

The need to reduce the weight of everyday use products and components has become crucial due to the exponential growth of human activities and their environmental impact. This reduction is necessary to minimize the carbon footprint and overall raw material usage. Among the sectors most affected by this issue are the automotive and aviation industries.<sup>1</sup> These industries are increasingly turning to expanded materials as a promising solution, primarily due to their properties such as low weight, multiple impact resistance, and excellent energy absorption, as well as thermal and acoustic characteristics.<sup>2–4</sup> Foams

are versatile multiphase materials which find application in a variety of industrial fields (such as sports equipment, furniture, footwear, and packaging).<sup>5</sup> Moreover, foams have found interesting applications beyond these fields. They are being used in separation processes, tissue engineering for bone reconstruction, and controlled drug release in pharmaceutical and nutraceutical applications. This demonstrates the broad range of uses for foams and their potential in diverse areas.<sup>6–8</sup>

Gas foaming is the most commonly used technique for producing foams, primarily because of its high productivity and versatility. The critical step in the gas foaming process is the solubilization of a blowing agent

This is an open access article under the terms of the [Creative Commons Attribution-NonCommercial](https://creativecommons.org/licenses/by-nc/4.0/) License, which permits use, distribution and reproduction in any medium, provided the original work is properly cited and is not used for commercial purposes.

© 2023 The Authors. *Journal of Applied Polymer Science* published by Wiley Periodicals LLC.

(BA) in the chosen thermoplastic polymer. When the BA/thermoplastic polymer solution is subjected to a specific process temperature and BA pressure, it reaches a thermodynamic equilibrium after a certain amount of time. The time required to achieve polymer saturation depends on the mutual properties of the BA and thermoplastic polymer, which regulate the mass transport during sorption, including diffusivity. Foaming takes place when the solution undergoes a thermodynamic instability, causing the polymer to become supersaturated. The release of the BA triggers the nucleation and growth of bubbles, leading to the formation of the expanded structure of the foam.<sup>9</sup>

Among the several BAs alternatives, the most employed eco-friendly solution in gas foaming processing is carbon dioxide, which is non-toxic, non-explosive, and easy to handle, providing an overall favorable interaction with most polymers.<sup>10,11</sup> Polymer foaming using carbon dioxide is a green process that finds application in a variety of fields.<sup>12</sup> Other gases as nitrogen, helium, and mixtures are employed.<sup>9,13–15</sup> The gas foaming and supercritical assisted foaming techniques<sup>16–18</sup> can be applied to standard industrial processes such as injection molding, extrusion, thermoforming, and batch processing. Batch foaming is also employed at the lab scale to optimize the foaming conditions and provide data for the scale-up of the process to the industrial level. Foaming techniques have been developed to process several thermoplastic polymers such as thermoplastic polyurethane, polystyrene, polyethylene, polyvinyl chloride, and many others<sup>19–21</sup> to meet the specific requirements of different industrial sectors. Recently, foamed plastics are demanded to possess some properties like flame retardancy, thermal stability, and mechanical strength to replace high-performance components.

In the aerospace and automotive industry, polysulfones (PSU)<sup>22</sup> and polyphenyl sulfones (PPSU) have attracted great attention due to their high stability, excellent aging resistance, low humidity absorption, high mechanical resistance, high chemical resistance, high hydrolytic stability, and rigidity.<sup>23–25</sup> PPSU, in particular, has been implemented in the manufacturing of aircraft interior elements,<sup>26</sup> in order to reduce the overall weight and improve the soundproof performance.<sup>27</sup> Moreover, PSU has built-in flame retardancy properties as required for aerospace applications, while PPSU complies with the Federal Aviation Administration requirements such as smoke release, heat generation, and toxicity.<sup>28–30</sup> Therefore, the use of PPSU is currently aimed at producing foams as core material in lightweight and heat-resistant sandwich structures.

For these reasons, the foaming of PSU has been studied in several scientific works. As an example, Guo et al. observed the structure and pore size of microcellular and nanocellular PSU foams as a function of the

CO<sub>2</sub> concentration.<sup>31</sup> Hu et al. investigated the microcellular foaming of PSU under different conditions and by employing co-BAs to improve the expansion ratio.<sup>32</sup> Bernardo et al. studied PPSU foamed samples and correlated the parameters of the autoclave gas foaming process to the resulting nanostructures.<sup>33</sup> Itoh and Kabumoto investigated the foaming behavior of PPS samples as a function of their crystallization temperatures in temperature rise foaming experiments.<sup>34</sup> Sorrentino et al. explored the foamability of PPSU, and other high-performance thermoplastic materials, under different conditions both by batch and solid-state foaming.<sup>35,36</sup> Summarizing, literature reports a PPSU reduction in density from 1.3 g/cm<sup>3</sup> to a range of 0.45–0.6 g/cm<sup>3</sup>. For this reason, the challenging aim is to reduce the weight even more using BAs such as carbon dioxide, nitrogen, or helium.

Therefore, this work was aimed at finding the most suitable operating conditions (sorption temperature, BA concentration, expansion rate, and sorption time) to maximize the expansion ratio of PPSU slab samples processed by batch gas foaming to obtain low-density and uniform microcellular structures. A second goal of the study was to guarantee the foamed PPSU slabs a regular shape in order to provide samples for further mechanical characterization. The experiments were divided into three sections: first, sorption tests were performed at low sorption times; then, confined foaming tests were performed during long-term saturation experiments. Finally, optimized conditions were sought, aiming to maximize the expansion ratio. Scanning electron microscopy (SEM) analysis was performed on a selection of the produced samples, to observe the cellular shape, the cells' mean dimensions and average cellular number density.

## 2 | MATERIALS AND METHODS

### 2.1 | Materials

Carbon dioxide, nitrogen, and helium were provided by Sol S.p.A., Monza, Italy. These gases have been used as BA in the range of pressures between 35 and 187 bar; for this reason, in case of operating pressure values higher than storage pressure, a Nex10 pump (Supercritical Fluid Technologies Inc, USA) has been used.

Radel R-5100 PPSU was kindly provided by Solvay, Belgium. The PPSU datasheet reported in Table 1 is updated on January 2021.

### 2.2 | Foaming equipment

The full experimental campaign has been performed using a foaming equipment working in batch mode. This

TABLE 1 Main properties of polyphenyl sulfone (PPSU).

Property	Value
Density	1300 kg/m <sup>3</sup>
Tensile modulus	2340 MPa
Tensile elongation break	7.6%
Glass transition temperature	220°C
Thermal conductivity	0.35 W/m K
Refractive index	1.672
Drying temperature	149°C
Drying time	2.5 h

process is characterized by a high-pressure autoclave equipped with a heating system and sensors for the simultaneous control of temperature and pressure; since this equipment has been standardized for different applications, it has been used to process several polymers with much different properties.<sup>37</sup> In this study, in order to saturate PPSU, the experiments were performed by injecting carbon dioxide, helium, or nitrogen, under a range of pressures among 35 and 187 bar, and temperatures among 200 and 260°C, thus creating sub-critical or supercritical conditions within the autoclave. In order to reach pressure values higher than storage pressure, a Nex10 pump (Supercritical Fluid Technologies Inc, USA) has been employed to reach steady-state conditions for foaming.

In detail, the foaming equipment is characterized by a pressurized reactor (0.3 L internal volume, HiP, model BC-1), an electrical heater controlled through a PID PLC (Gefran 1850), a pressure transducer (Gefran TK), a discharge ball valve (HiP, model 15–71 NFB), an electromechanical actuator (HiP, model 15–72 NFB TSR8), and an electrovalve. The pressure and temperature data were collected using a data acquisition system (Gefran GF\_eXpress).

## 2.3 | Methods

### 2.3.1 | Diffusivity tests

For this first set of experiments, a rectangular slab (40 × 40 × 5 mm<sup>3</sup>) of PPSU was placed in a 40 × 40 × 10 mm<sup>3</sup> mold. The experiments grouped in the first section were focused on estimating gas apparent diffusivity (i.e., an estimation of the order of magnitude of diffusion of gas molecules) in PPSU during a short sorption time (set at 5 min). The diffusivity was in fact estimated by the measurement of the BAs penetration depth in the sample by optical instruments. In particular, the defined sorption time was set to be

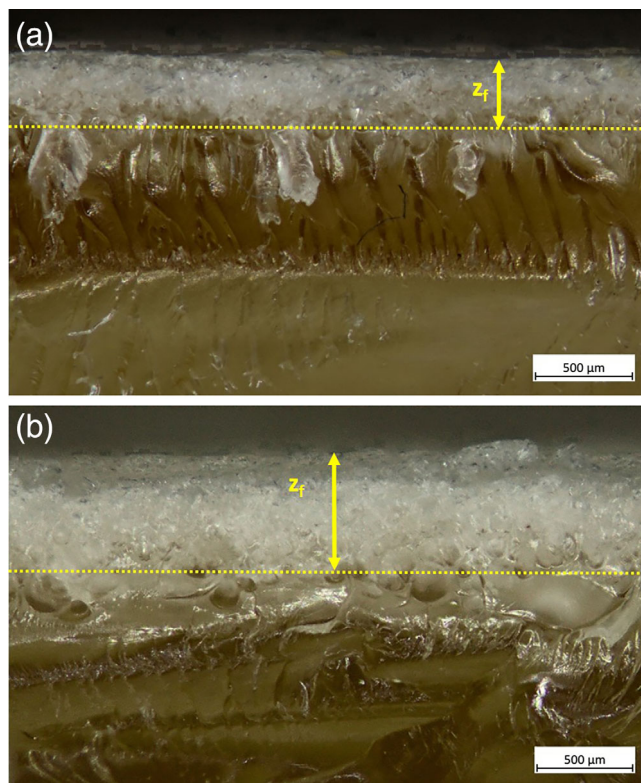


FIGURE 1 Microscopy observations of polyphenyl sulfone (PPSU) foamed with CO<sub>2</sub> at 220°C (a) and 240°C (b). [Color figure can be viewed at [wileyonlinelibrary.com](https://onlinelibrary.wiley.com/doi/10.1002/app.54574)] See the Terms and Conditions (<https://onlinelibrary.wiley.com/terms-and-conditions>) on Wiley Online Library for rules of use; OA articles are governed by the applicable Creative Commons License

significantly lower than the characteristic time to reach saturation between 200 and 260°C.

During these preliminary experiments, it was possible to measure the foamed thickness of the processed slabs ( $z_f$ ), thus allowing estimation of the diffusivity of CO<sub>2</sub> in the PPSU slab, in each explored operating condition. These measurements were performed by observing a section of the PPSU slab using a trinocular stereomicroscope, Optika mod. SZX-T, Optikamicroscopes, Ponteranica (BG), Italy, equipped with a C-B3A camera 3 Mpx. Samples were cut along their section and observed without any further preparation (Figure 1). Considering  $z_f$  as the average thickness of the foamed layer, the length of the not expanded layer was calculated as  $L_{NE} = z_a - 2 z_f$ , being  $z_a$  the average thickness of PPSU after the foaming process. According to this first experimental campaign, the estimation of the saturation time for PPSU using CO<sub>2</sub> ranged between 57 h at 200°C and 1.5 h at 260°C.

A repeatability analysis has been performed on a specific sample foamed at 220°C using CO<sub>2</sub> as BA. In detail, three slabs of the same polymer have been processed at the same operating conditions, thus obtaining similar measurements of apparent diffusivity. Therefore, the apparent diffusivity values have been reported in Table 2 as averages with negligible standard deviations.

TABLE 2 Diffusivity tests at 75 bar for a sorption time of 5 min, using CO<sub>2</sub>, N<sub>2</sub>, and He as blowing agents.

Blowing agent	Temperature, °C	$z_f$ , $\mu\text{m}$	Apparent diffusivity, $\text{m}^2/\text{s}$	$\varphi_g$ , %
CO <sub>2</sub>	220	313 ± 35	8.2E-11	199
CO <sub>2</sub>	230	362 ± 68	1.2E-10	188
CO <sub>2</sub>	235	450 ± 65	2.5E-10	164
CO <sub>2</sub>	240	546 ± 41	4.9E-10	142
CO <sub>2</sub>	245	632 ± 70	3.3E-10	199
CO <sub>2</sub>	250	642 ± 145	5.7E-10	156
CO <sub>2</sub>	255	914 ± 123	9.5E-10	171
CO <sub>2</sub>	260	1159 ± 129	1.1E-09	198
N <sub>2</sub>	220	272 ± 46	2.5E-10	101
N <sub>2</sub>	230	664 ± 68	6.7E-10	150
N <sub>2</sub>	240	855 ± 56	1.7E-09	120
N <sub>2</sub>	250	1127 ± 82	2.5E-09	131
N <sub>2</sub>	260	1352 ± 153	4.8E-09	113
He	220	1121 ± 42	3.9E-09	103
He	230	$z_f > \text{thickness}$	$D > 2.1\text{E-}08$	111
He <sup>a</sup>	230	$z_f > \text{thickness}$	$D > 5.2\text{E-}08$	102

<sup>a</sup>Experiment with a sorption time of 2 min.

With the aim of showing the technique employed for the measurement of the foamed layer, as an example, two samples' sections produced using CO<sub>2</sub> at 220 and 240°C, respectively, were shown in Figure 1.

This set of experiment resulted in defining the exact sorption time needed to saturate the PPSU samples in order to obtain uniform foaming.

### 2.3.2 | Confined foaming

The second set of experiments was performed using the same PPSU slab geometry (40 × 40 × 5 mm<sup>3</sup>); also in this case, the mold had a cavity of the same geometry but twice the thickness of the sample. Under these conditions, the polymer expansion was forced to occur only in the slab thickness direction. In this context, confined expansion occurred, meaning that the polymer was limited to expand to about twice its volume at most (mold thickness of 10 mm). Tests were performed at saturation sorption times previously calculated in the previous set of experiments (see Section 2.3.1).

### 2.3.3 | Unconfined foaming

Following the path defined by the best optimized conditions of pressure and temperature, the third batch of experiments

consisted of unconfined expansion tests of PPSU pieces (with irregular geometries), having a total volume at least 5 times smaller than the total volume of the mold cavity (40 × 40 × 10 mm<sup>3</sup>). In this last case, the PPSU slab was free to expand in each direction inside the mold, thus obtaining even larger final volumes and, hence, lower density values. This final test was aimed at finding comparison among the effect of carbon dioxide, nitrogen, and helium, also in terms of cell density and isotropic factor of cells.

The dimensions of each PPSU slab were measured before and after the gas foaming process. In particular,  $z_b$  is defined as the initial thickness of the overall PPSU slab, measured before gas foaming, while  $z_a$  is the average thickness of PPSU after the foaming process and  $z_f$  is the average measured thickness of the foamed layer. Foaming experiments were produced in triplicate.

### 2.3.4 | Calculations

The penetration thickness of the BA (i.e., the depth penetration of the BA during sorption) was calculated using Equation (1):

$$\delta = \frac{z_b - L_{NE}}{2} = \frac{z_b - z_a + 2z_f}{2}, \quad (1)$$

where  $L_{NE}$  is the length of the not expanded layer.

The geometrical expansion ratio ( $\varphi_g$ ) of the polymer, obtained using the measured foamed thickness, was calculated as:

$$\varphi_g(\%) = \frac{\delta}{(z_f/2)} * 100. \quad (2)$$

In the case of confined and unconfined expansion, the expansion ratio is determined as the ratio of densities before ( $\rho_i$ ) and after ( $\rho_f$ ) the foaming process.

$$\varphi = \frac{\rho_i}{\rho_f}. \quad (3)$$

Sorption time  $t_s$  being the diffusivity of the gas can be determined by

$$t_s = \frac{\delta^2}{D}, \quad (4)$$

where  $D$  is gas diffusivity at the working conditions of pressure and temperature and  $\delta$  is the penetration thickness as defined above.

Foamed samples were also characterized using SEM (mod. Merlin VP compact, Zeiss, Germany). Using Fiji software, cell number density was obtained from SEM images, indicated as the number of cells nucleated per unit volume of the original unfoamed polymer PPSU ( $N_0$ )<sup>31</sup>:

$$N_0 = \left(\frac{n}{A}\right)^{3/2} \frac{1}{1 - V_f}, \quad (5)$$

where  $n$  represents the number of cells in the SEM image; according to the correlations reported in the literature,<sup>31</sup>  $A$  is the area of the micrograph, and  $V_f$  is the void fraction of foam, calculated as:

$$V_f = 1 - \frac{\rho_f}{\rho_i} \quad (6)$$

An isotropic factor for the cells was calculated as the average length ratio along the two orthogonal directions ( $L_1$  and  $L_2$ ) of the cell walls.

$$IF = \frac{L_1}{L_2} * 100\%. \quad (7)$$

### 3 | RESULTS

#### 3.1 | Diffusivity tests

In the first set of experiments, the BA apparent diffusivity was estimated through gas sorption at 75 bar for 5 min,

with the specific aim not to achieve slab saturation (see Section 2.3). The experiments were carried out at temperatures ranging between 220 to 260°C. Table 2 reports the processing parameters and results of apparent diffusivity tests performed using carbon dioxide, nitrogen, and helium.

Figure 2 compares values of apparent diffusivity for all explored temperature conditions. In particular, Arrhenius fitting curves have been drawn over experimental points obtained for carbon dioxide and nitrogen.

The results demonstrated that the apparent diffusivity of carbon dioxide in PPSU increases with temperature in the explored range. In particular, an Arrhenius behavior was observed with an average activation energy of diffusivity ( $E_d$ ) of about 144.8 kJ/mol for carbon dioxide and of 158.4 kJ/mol for nitrogen.

Using this average value of activation energy, apparent diffusivity values at 200 and 210°C were estimated, obtaining, respectively, 3.1E-11 and 5.9E-11 m<sup>2</sup>/s. These two conditions are below the PPSU's glass transition temperature; therefore, they were extrapolated by the model and not obtained experimentally, since the diffusion test would not result in a macroscopic foamed thickness to measure easily (see Section 2.3). At 220°C, the diffusivity was 8.2E-11 m<sup>2</sup>/s, which corresponded to a foamed thickness of 313 ± 35 μm; this value increases almost by an order of magnitude, up to 4.9E-10 m<sup>2</sup>/s, at 240°C, corresponding to a foamed thickness of 546 ± 41 μm. At the highest explored

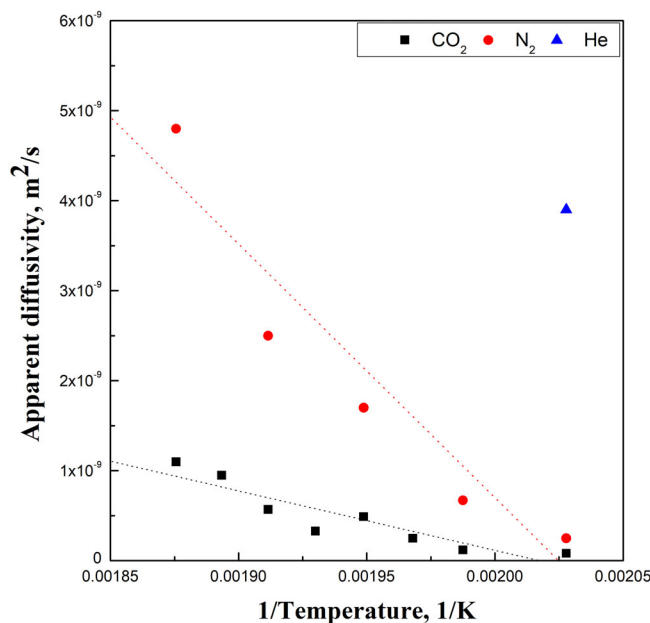


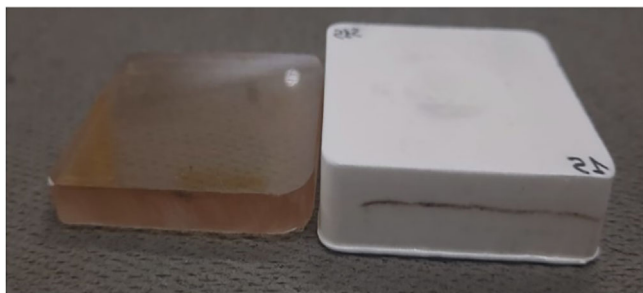
FIGURE 2 Diffusivity of CO<sub>2</sub>, N<sub>2</sub>, and He in polyphenyl sulfone (PPSU) slabs fitted using Arrhenius correlation. [Color figure can be viewed at [wileyonlinelibrary.com](http://wileyonlinelibrary.com)]

temperature (260°C), the value of  $z_f$  was  $1159 \pm 129 \mu\text{m}$ , while diffusivity reached  $1.1\text{E-}09 \text{ m}^2/\text{s}$ .

As represented in Figure 2, carbon dioxide and nitrogen show a quite similar apparent diffusivity trend in the range 220–260°C at 75 bar. However, for nitrogen, the effect of temperature is more evident. According to the available literature about PPSU,  $\text{CO}_2$  apparent diffusivity in PPSU is reported in ranges between  $1\text{E-}11$  and  $3\text{E-}11 \text{ m}^2/\text{s}$  while operating in the range 60–300 bar, with density values between 600 and  $800 \text{ kg}/\text{m}^3$  in the range 150–220°C,<sup>33</sup> and among  $4.5\text{E-}10$  and  $9.5\text{E-}10 \text{ m}^2/\text{s}$  in the operative ranges of 40–60°C and 200–400 bar.<sup>38</sup> The actual literature on BA apparent diffusivity in PPSU systems is focused mainly on carbon dioxide, explored in different thermodynamic conditions; there is some data about nitrogen<sup>39</sup> apparent diffusivity in PPSU at 20°C and 1 bar ( $1.2\text{E-}12 \text{ m}^2/\text{s}$ ), but no dataset or publications report helium apparent diffusivity measurements.

In the last two cases reported in Table 2, regardless of the short sorption time, the samples were saturated by the BA. Therefore, the calculation of helium apparent diffusivity (i.e., the penetration depth of the gas in the PPSU slab) was not possible since, in these cases,  $z_f$  was equal to  $z_a$ . As a consequence, helium diffusivity was estimated to be larger than the minimum theoretical diffusivity value required to saturate the whole thickness of the PPSU slab in 5 and 2 min, respectively.

Samples produced at 240°C or lower showed a rectangular-like section shape, similar to the original PPSU slab (see Figure 1). In these cases, it was notably straightforward to differentiate between the thickness of the foamed layer (white-opaque) and the unexpanded core (orange-ocher). On the other hand, by foaming at 250 and 260°C, an irregular and complex section was obtained, due to the lower viscosity of the polymer. Therefore, the following temperature conditions were set at values lower than 240°C, in order to produce regular shapes.

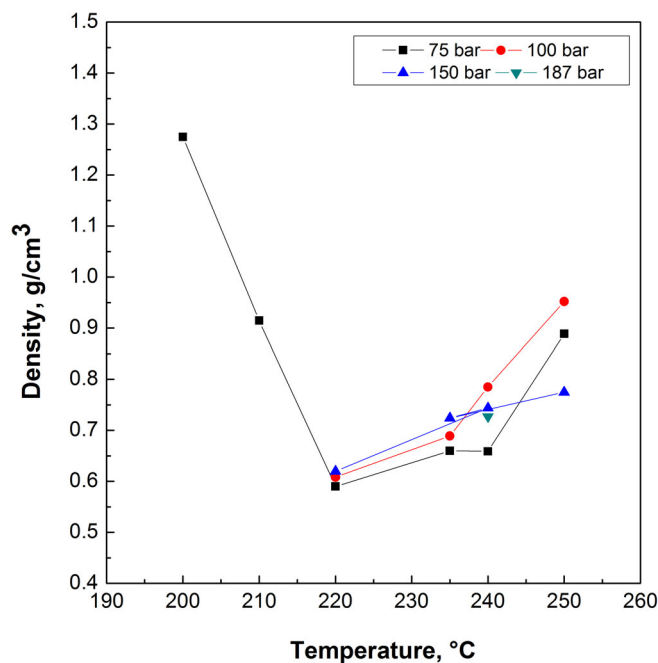


**FIGURE 3** Example of confined foaming experiment before (left) and after (right) the foaming process. [Color figure can be viewed at [wileyonlinelibrary.com](http://wileyonlinelibrary.com)]

### 3.2 | Confined expansion tests

Figures 3 and 4 and Tables 3 and 4 report the results obtained using carbon dioxide at different ranges of pressure (35–187 bar) and temperature (200–240°C). For the experiments of the second section, the minimum sorption time to achieve saturation was calculated according to the results of the diffusivity tests (Section 3.1, Table 2), and the proposed Arrhenius model, for each temperature and pressure condition.

The diffusivity tests performed using carbon dioxide as BA allowed the estimation of the sorption time for the saturation of PPSU slabs with a thickness of 5 mm, operating in the range of temperatures between 200 and 260°C (see Table 2). Considering the diffusivity values fitted using the Arrhenius model, the sorption time calculated for each experimental condition allowed the saturation of PPSU slabs around glass transition temperature (220°C) and at 75–100 bar. Therefore, saturation can be obtained even at higher temperatures shown in Table 3. As expected, below the glass transition temperature (i.e., at 200 and 210°C), the  $\phi$  was equal to 102% and 132%, respectively, resulting in an unfoamed or slightly foamed sample. Instead, operating 220°C and at higher temperatures,  $\phi$  increased ranging from a minimum of 166% to a maximum of 211%. A comparative test using carbon dioxide has been performed at 35 bar and 220°C, resulting in an unfoamed sample, probably due to a reduced amount of



**FIGURE 4** Foam density as a function of foaming temperature at different operating pressures. [Color figure can be viewed at [wileyonlinelibrary.com](http://wileyonlinelibrary.com)]

solubilized BA, compared to the other tests, and, moreover, a reduced plasticizing effect. While, samples foamed between 220 and 240°C at 75 and 100 bar, exhibited a  $\varphi$  between 170 and 200 and maintained a regular square shape. Further increase of the operating pressure did not cause noticeable effects. At temperatures higher 220°C, the lower viscosity of PPSU affects the stability of the cell walls and entails, in addition, the development of shape irregularities. Figure 3 shows a PPSU sample before (left) and after (right) the foaming process when obtaining a  $\varphi$  equal to 211% (see Table 4). After the foaming process, the PPSU slab became opaque and its thickness doubled.

**TABLE 3** Confined expansion experiments using CO<sub>2</sub> as the blowing.

Temperature, °C	Pressure, bar	Density, kg/m <sup>3</sup>	$\varphi$ , %
200	75	1280	102
210	75	975	132
220	35	1230	107
220	75	590	190
220	100	610	211
220	150	651	200
235	75	660	197
235	100	690	183
235	150	720	175
240	75	660	197
240	100	790	166
240	150	740	175
240	187	730	176

**TABLE 4** Confined/unconfined expansion tests at 100 bar and 220 and 230°C with CO<sub>2</sub>, N<sub>2</sub>, and He.

Blowing agent	Type of expansion	Temperature, °C	Density, kg/m <sup>3</sup>	$\varphi$ , %
CO <sub>2</sub>	Confined	220	610	211
N <sub>2</sub>	Confined	220	1210	106
He	Confined	220	1280	101
CO <sub>2</sub> + N <sub>2</sub> <sup>a</sup>	Confined	220	885	147
CO <sub>2</sub>	Unconfined	220	320	391
CO <sub>2</sub>	Unconfined	230	340	386
N <sub>2</sub>	Unconfined	220	1100	104
N <sub>2</sub>	Unconfined	230	900	147
He	Unconfined	220	1240	111
He	Unconfined	230	960	133

<sup>a</sup>CO<sub>2</sub> + N<sub>2</sub> means a gaseous mixture of carbon dioxide at 20% over nitrogen at 80%.

Figure 4 shows the density values of the foamed PPSU slabs as a function of temperature, as the operating pressure varies.

The effect of operating temperatures ranging from 200 to 240°C was explored (Figure 4), thus obtaining a minimum value of density at of about 600 kg/m<sup>3</sup>, corresponding to the temperature of 220°C for all the explored operating pressures. In conclusion, the optimal sorption conditions when using carbon dioxide as BA were set as 220°C and 100 bar.

Considering the negligible variation of  $\varphi$  as the operating pressure varies (see Table 3), the following confined foaming experiments were performed at 100 bar. Further experiments were carried out by using nitrogen and helium as alternative BAs and operating under the optimized sorption conditions established with carbon dioxide as BA.

### 3.3 | Unconfined expansion tests

In this section, the results of unconfined expansion tests (see Section 2.3). at a pressure of 100 bar and temperatures of 220 and 230°C, are reported for each BA. These experiments were aimed at allowing the samples to reach the maximum  $\varphi$  at the optimized foaming conditions. The reduced volume of the slabs (five times lower, see Section 2.3) allowed the expansion of the samples in the three directions without limitations. The effect of different values of sorption temperatures was explored in order to attest to the stability of the process and to confront the  $\varphi$  values evaluated in the previous sections (Table 4).

Carbon dioxide confined expansion resulted in a  $\varphi$  value of 211%, with a density of 610 kg/m<sup>3</sup>. Operating

under the same conditions for unconfined expansion, the  $\varphi$  reached 391%, with a minimum density of 320 kg/m<sup>3</sup> and a volumetric ratio of about 25.5%, becoming almost a quarter of the initial 1300 kg/m<sup>3</sup>. Increasing the temperature to 230°C, an  $\varphi$  of 386% was reached.

At the same operating conditions, confined expansion using nitrogen resulted in a  $\varphi$  of 106% with a density of 1210 kg/m<sup>3</sup>, while it gave a similar result in the case of unconfined expansion with  $\varphi$  of 104% and a density of 1100 kg/m<sup>3</sup>. However, at 230°C, the  $\varphi$  reached 147% with a density of 900 kg/m<sup>3</sup>.

A gaseous mixture of BAs (20% CO<sub>2</sub> and 80% N<sub>2</sub>) was also used to study the simultaneous effect of carbon dioxide and nitrogen in confined foaming experiments. As it was expected, the density reached was 885 kg/m<sup>3</sup>, as well as the expansion ratio of 147%, included among 211% obtained with pure CO<sub>2</sub> and 106% with pure N<sub>2</sub>.

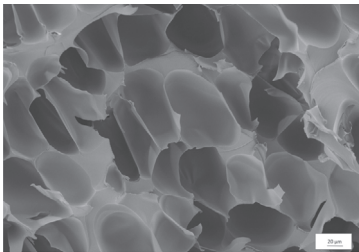
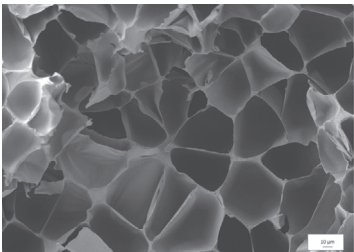
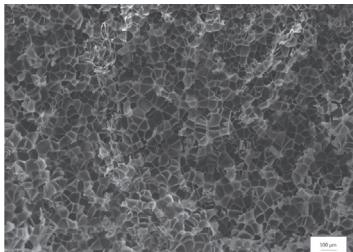
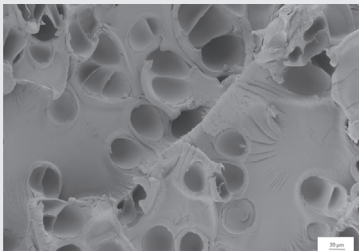
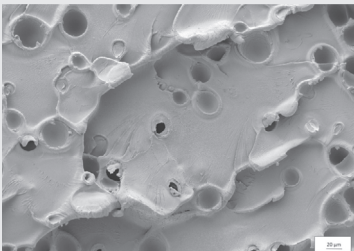

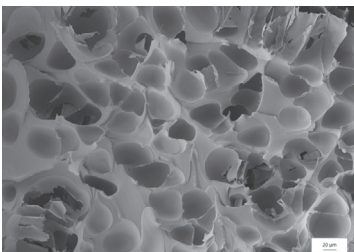
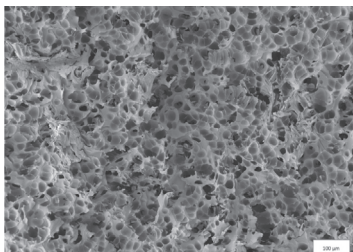
Also in the last case, helium showed low foaming ability at the optimized conditions for carbon dioxide, resulting in a value of  $\varphi$  of 111% and 1240 kg/m<sup>3</sup> at 220°C, up to a maximum of 133%  $\varphi$  and a minimum of 960 kg/m<sup>3</sup> density.

### 3.4 | SEM analysis

To explore the PPSU foamed samples' cellular structure, SEM analysis was employed. The analysis was aimed at highlighting the effect of both confined and unconfined conditions on the expanded polymers. Therefore, in Table 5, some cross sections of PPSU slabs obtained at confined and unconfined foaming conditions have been reported for the different BAs used.

The images obtained by SEM were then analyzed by using Fuji analysis software.<sup>40</sup> For each analyzed sample, the number of nucleated cells per unit volume has been calculated, as well as the cells' mean size and isotropic factor. Results are reported in Table 6. To calculate cell density with minimized error, SEM images with lower magnitudes were also reported and analyzed. These microcellular foams show some differences in terms of cell morphology. For instance, the use of carbon dioxide created ellipsoidal cells in confined conditions, while, irregular cells in unconfined conditions; tests performed by using helium and nitrogen as BAs resulted in the formation of more round and homogeneous cells.

TABLE 5 SEM images of PPSU slabs foamed using CO<sub>2</sub>, N<sub>2</sub>, and He (confined/unconfined conditions).

BA	Confined, ×250	Unconfined, ×300	Unconfined, ×50
CO <sub>2</sub>			
N <sub>2</sub>			
He	Not foamed		

Abbreviations: BA, blowing agent; PPSU, polyphenyl sulfone; SEM, scanning electron microscopy.



TABLE 6 Mean dimensions, density, and isotropic factor (IF) of cells obtained under confined and unconfined expansion.

Blowing agent	Type of expansion	Temperature, °C	Pressure, bar	Mean size, $\mu\text{m} \pm \text{SD}$	Cell number density, $\#/\text{cm}^3$	IF, %
CO <sub>2</sub>	Confined	220	100	78 $\pm$ 19	0.3E07	59.7
N <sub>2</sub>	Confined	220	100	39 $\pm$ 8	2.5E05	74.6
CO <sub>2</sub> + N <sub>2</sub> <sup>a</sup>	Confined	220	100	45 $\pm$ 9	5.4E05	81.4
CO <sub>2</sub>	Unconfined	220	100	44 $\pm$ 10	1.3E07	85.8
N <sub>2</sub>	Unconfined	220	100	38 $\pm$ 10	2.6E05	83.2
He	Unconfined	230	100	50 $\pm$ 16	1.8E06	86.6

<sup>a</sup>CO<sub>2</sub> + N<sub>2</sub> means a gaseous mixture of carbon dioxide at 20% over nitrogen at 80%.

Recalling data shown in Table 4, the use of carbon dioxide as a BA for the PPSU foaming process resulted in a  $\varphi$  of 211% for confined expansion and almost 400% for unconfined expansion, in the best operating conditions. In the first case, an isotropic factor of about 60% was measured, probably because PPSU slabs were confined along two dimensions and were able to expand following the third preferential one, as confirmed by SEM images reported in Table 6. Indeed, the mean size of cells measured directly on SEM images, was 78  $\pm$  19  $\mu\text{m}$  for confined carbon dioxide expansion, with a cell density of 0.3E07 cells/cm<sup>3</sup>. In the case of unconfined expansion, the cell mean size was 44  $\pm$  10  $\mu\text{m}$ , while the isotropic factor increased up to 85.8%, being consistent with a more homogeneous expansion in all directions. Moreover, the cell density increased by about 4.2 times, up to a value of 1.3E07 cells/cm<sup>3</sup>.

Concerning nitrogen used as the BA, the  $\varphi$  was equal to 106% in the case of confined expansion, and 104% for unconfined expansion, thus no influence by the process conditions were observed. The reduced  $\varphi$  resulted in a larger isotropic factor (74.6%) and smaller cell dimensions of 39  $\pm$  8  $\mu\text{m}$ , with a cell density of 2.5E05 cells/cm<sup>3</sup>. This value remained practically similar if compared to the case of unconfined expansion, with a cell density of 2.6E06 cells/cm<sup>3</sup> and an isotropic factor of 83.2%.

Concerning the sample processed using a gaseous mixture of BAs (20% CO<sub>2</sub> and 80% N<sub>2</sub>), it was possible to measure cell mean size of 45  $\pm$  9  $\mu\text{m}$  and a cell number density of 5.4E05 cells/cm<sup>3</sup>. As expected for density, also mean size and cell density were characterized by an intermediate value among pure CO<sub>2</sub> foaming and pure N<sub>2</sub> foaming. Surprisingly, isotropic factor was 81.4%, larger than pure carbon dioxide and nitrogen foaming confined experiments.

Confined expansion using helium as BA did not produce any visible observation of cells and was omitted from Table 6. Only unconfined expansion performed at 230°C with helium, used as the BA, has been considered.

In this case,  $\varphi$  was 133%, corresponding to a mean cell dimension of 50  $\pm$  16  $\mu\text{m}$ , and to a cell density of 1.8E06 cells/cm<sup>3</sup>, which is a larger value than the one found for nitrogen foamed slabs. The isotropic factor was 86.6%, in accordance with the one obtained for the other BAs.

According to the literature study, there are still some challenges in order to process PPSU to obtain foams, depending on the process employed and to the conditions explored. Therefore, solid-state foaming<sup>31</sup> was employed, obtaining an expansion ratio among 110 and 400%. Using ethanol as co-BA, batch foaming was employed to obtain expansion ratio of 502% using carbon dioxide as BA.<sup>32</sup> According to the literature, PPSU and PSU were foamed using compression molding technique at 280 and 250°C, respectively, with a slab thickness of 1.5 mm,<sup>32</sup> obtaining saturation at similar sorption time of this work, but a reduced cell average diameter and an increased cell number density. This is due to the different process employed; therefore, PPSU has been proven to present also nanometric cells (around 20 nm). Anisotropy related to PPSU foaming has not been deeply studied yet, but it is generally explained in terms of coalescence during the process.<sup>41</sup>

## 4 | CONCLUSIONS

This work was aimed at finding the best operating conditions to produce PPSU foamed slabs using a lab-scale gas foaming process at high pressure conditions. The first set of experiments confirmed the diffusivity of carbon dioxide in PPSU, as reported in the literature, while the tests performed using nitrogen and helium introduced, for the first time, apparent diffusivity measurements at high-pressure conditions.

The results obtained during the apparent diffusivity tests were used as guidelines for the following experiments of confined expansion of PPSU slabs. A wide range of temperatures and pressures were explored for carbon dioxide, finding the best operating conditions in correspondence to

the PPSU glass transition temperature of 220°C and at the pressure of 100 bar. Improving the processing conditions resulted in an expansion ratio ( $\varphi$ ) of 211%.

Comparative expansion tests were performed using helium and nitrogen as BAs, demonstrating lower expansion ratios ( $\varphi$ ) values. In the unconfined expansion tests,  $\varphi$  up to 391% and density equal to 320 kg/m<sup>3</sup> were obtained by carbon dioxide saturation, while helium and nitrogen demonstrated lower values.

The results presented in this study provide a basis to further investigate the effect of processing conditions on PPSU foam structures. The requirements of industrial sectors, such as aerospace and automotive, for lightweight and high-performance core materials, can be met by fine tuning the structure and properties of components made of expanded polyphenyl sulfone. In order to achieve this goal, the use of gaseous mixtures will be also employed in foaming experiments to exploit simultaneous hybrid effects of singular BAs such as carbon dioxide and nitrogen, resulting in intermediate diffusion properties.

## NOMENCLATURE

$z_b$	initial thickness of the overall PPSU slab measured before gas foaming
$z_a$	average thickness of PPSU slab after the foaming process
$z_f$	average thickness of the foamed layer
$L_{NE}$	length of the not expanded layer
$\delta$	depth penetration of the blowing agent during sorption
$\varphi_g$	geometrical expansion ratio
$\varphi$	expansion ratio calculated as densities ratio
$t_s$	sorption time of the blowing agent into the polymer
$D$	diffusivity
$\rho_f$	density of the foamed layer
$\rho_i$	initial density of not foamed PPSU polymer
$n$	number of cells reported in the micrograph
$A$	area of the SEM micrograph
$N_0$	cells nucleated per unit volume of the original unfoamed polymer PPSU
$V_f$	void fraction

## AUTHOR CONTRIBUTIONS

**Paolo Trucillo:** Conceptualization (equal); data curation (lead); investigation (equal); methodology (lead); software (lead); validation (lead); writing – original draft (equal).

**Fabrizio Errichiello:** Conceptualization (equal); data curation (supporting); formal analysis (supporting); investigation (equal); methodology (supporting); supervision (supporting); validation (equal); visualization (lead); writing – review and editing (equal). **Ernesto Di Maio:**

Conceptualization (equal); data curation (equal); formal analysis (lead); investigation (lead); methodology (supporting); project administration (lead); supervision (supporting); validation (supporting); visualization (supporting); writing – review and editing (equal).

## DATA AVAILABILITY STATEMENT

Research data are not shared.

## ORCID

Paolo Trucillo  <https://orcid.org/0000-0001-6255-6950>

Fabrizio Errichiello  <https://orcid.org/0000-0002-7333-5069>

Ernesto Di Maio  <https://orcid.org/0000-0002-3276-174X>

## REFERENCES

- [1] J. Bachmann, C. Hidalgo, S. Bricout, *Sci. China Technol. Sci.* **2017**, *60*, 1301.
- [2] N. Z. M. Zaid, M. R. M. Rejab, N. A. N. Mohamed, *MATEC Web Conf.* **2016**, *74*, 74.
- [3] J. Banhart, *Int. J. Veh. Des.* **2005**, *37*, 114.
- [4] G. Wang, G. Zhao, G. Dong, Y. Mu, C. B. Park, G. Wang, *Eur. Polym. J.* **2018**, *103*, 68.
- [5] E. Di Maio, E. Kiran, *J. Supercrit. Fluids* **2018**, *134*, 157.
- [6] M. Champeau, J. M. Thomassin, T. Tassaing, C. Jérôme, *J. Controlled Release* **2015**, *209*, 248.
- [7] P. Sepulveda, J. R. Jones, L. L. Hench, *J. Biomed. Mater. Res.* **2002**, *59*, 340.
- [8] R. K. Prud'homme, G. G. Warr, in *Foams*, Routledge, New York **1996**, p. 551.
- [9] E. Di Maio, S. Iannace, G. Mensitieri, in *Foaming with Supercritical Fluids*, Vol. 9, Elsevier, Netherlands **2021**, p. 33.
- [10] F. L. Jin, M. Zhao, M. Park, S. Park, *J. Polym.* **2019**, *11*, 953.
- [11] M. Sauceau, J. Fages, A. Common, C. Nikitine, E. Rodier, *Prog. Polym. Sci.* **2011**, *36*, 749.
- [12] I. Tsivintzelis, G. Sanxaridou, E. Pavlidou, C. Panayiotou, *J. Supercrit. Fluids* **2016**, *110*, 240.
- [13] A. Wong, L. H. Mark, M. M. Hasan, C. B. Park, *J. Supercrit. Fluids* **2014**, *90*, 35.
- [14] A. Wong, S. Leung, M. Hasan, C. B. Park, presented at Reg. Tech. Conf. Soc. Plast. Eng., Vol. 4 **2008**, p. 2534.
- [15] C. Yu, Y. Wang, B. Wu, Y. Xie, C. Yu, S. Chen, W. Li, *Polym. Test.* **2011**, *30*, 887.
- [16] D. L. Tomasko, A. Burley, L. Feng, S. K. Yeh, K. Miyazono, S. Nirmal-Kumar, I. Kusaka, K. Koelling, *J. Supercrit. Fluids* **2009**, *47*, 493.
- [17] L. J. M. Jacobs, M. F. Kemmere, J. T. F. Keurentjes, *Green Chem.* **2008**, *10*, 731.
- [18] E. Reverchon, S. Cardea, *J. Supercrit. Fluids* **2007**, *40*, 144.
- [19] K. C. Khemani, *ACS Symp. Ser.* **1997**, *669*, 1.
- [20] K. C. Frisch, *J. Macromol. Sci. Part A Chem.* **1981**, *15*, 1089.
- [21] R. Gautam, A. S. Bassi, E. K. Yanful, *Appl. Biochem. Biotechnol.* **2007**, *141*, 85.
- [22] Z. Li, Y. Jia, S. Bai, *RSC Adv.* **2018**, *8*, 2880.
- [23] Y. Wang, R. P. Górecki, E. Stamate, K. Norrman, D. Aili, M. Zuo, W. Guo, C. Hélix-Nielsen, W. Zhang, *RSC Adv.* **2019**, *9*, 278.
- [24] H. Sun, G. S. Sur, J. E. Mark, *Eur. Polym. J.* **2002**, *38*, 2373.

- [25] Y. Liu, X. Yue, S. Zhang, J. Ren, L. Yang, Q. Wang, G. Wang, *Sep. Purif. Technol.* **2012**, 98, 298.
- [26] T. S. Williams, B. Nguyen, W. K. Fuchs, M. Kelly, presented at Int. SAMPE Tech. Conf., June **2021**, p. 79.
- [27] V. Kumar, P. S. Yeole, N. Hiremath, R. Spencer, K. M. M. Billah, U. Vaidya, M. Hasanian, M. Theodore, S. Kim, A. A. Hassen, V. Kunc, *Compos. Sci. Technol.* **2021**, 201, 108525.
- [28] E. M. Pearce, *Am. Chem. Soc. Polym. Prepr. Div. Polym. Chem.* **1985**, 26, 198.
- [29] F. Jia, M. K. Patel, E. R. Galea, A. Grandlson, J. Ewer, *Aeronaut. J.* **2006**, 110, 303.
- [30] R. E. Lyon, T. Emrick, *Polym. Adv. Technol.* **2008**, 19, 609.
- [31] H. Guo, A. Nicolae, V. Kumar, *Cell Polym.* **2016**, 35, 119.
- [32] D. Hu, Y. Gu, T. Liu, L. Zhao, *J. Supercrit. Fluids* **2018**, 140, 21.
- [33] V. Bernardo, J. Martín-De León, M. A. Rodríguez-Pérez, *Mater. Lett.* **2016**, 178, 155.
- [34] M. Itoh, A. Kabumoto, *Furukawa Rev.* **2005**, 56, 32.
- [35] M. Gargiulo, L. Sorrentino, S. Iannace, presented at AIP Conf. Proc., Vol. 1042 **2008**, p. 109.
- [36] L. Sorrentino, M. Aurilia, S. Iannace, *Adv. Polym. Technol.* **2011**, 30, 234.
- [37] C. Marrazzo, E. Di Maio, S. Iannace, L. Nicolais, *J. Cell. Plast.* **2008**, 44, 37.
- [38] M. Tang, Y. C. Huang, Y. P. Chen, *J. Appl. Polym. Sci.* **2004**, 94, 474.
- [39] F. Feng, C. Z. Liang, J. Wu, M. Weber, C. Maletzko, S. Zhang, T. S. Chung, *Polymer* **2021**, 13, 2745.
- [40] M. D. Abràmoff, P. J. Magalhães, S. Ram, *J. Biophotonics Int.* **2004**, 11, 36.
- [41] D. Cuadra-Rodríguez, S. Barroso-Solares, *J. Pinto Nanomater.* **2021**, 11, 621.

**How to cite this article:** P. Trucillo, F. Errichiello, E. Di Maio, *J. Appl. Polym. Sci.* **2023**, e54574. <https://doi.org/10.1002/app.54574>